JOURNAL OF AGRICULTURAL AND FOOD CHEMISTRY

Article

pubs.acs.org/JAFC

Charge Compensation, Phase Diagram, and Protein Aggregation in Soy Protein−Gum Arabic Complex Formation

Die Dong,[†] Yufei Hua,*[,†] Yeming Chen,[†] Xiangzhen Kong,[†] Caimeng Zhang,[†] and Qi Wang[§]

[†]State Key Laboratory of Food Science and Technology, School of Food Science and Technology, Jiangnan University, 1800 Lihu Avenue, Wuxi 214122, Jiangsu Province, People's Republic of China

[§]Guelph Food Research Centre, Agriculture and Agri-Food Canada, Guelph, Ontario N1G 5C9, Canada

ABSTRACT: Mixtures of soy protein (SP) and gum arabic (GA) formed an electrostatic complex in a relatively narrow pH range at very low ionic strength. The conditions under which the complexes could be formed were determined using turbidimetric measurements first. In salt-free condition and 1:1 SP/GA mixture, critical pH values with the formation of soluble (pH_c = 4.40), insoluble ($pH_{\varphi 1}$ = 3.55), and maximum (pH_{opt} = 3.15) complexes were observed. As SP/GA ratios increased from 1:4 to 8:1, critical pH values shifted toward higher pH. Charge densities (ZN) for SP and GA were calculated from electrophoretic mobility using soft particle analysis theory. Results showed that a 1:1 charge ratio at $pH_{\varphi 1}$ was found at any SP/GA ratio, indicating that charge compensation was fulfilled for SP/GA insoluble complex formation. A SP−GA−water ternary phase diagram was built at pH 4.0. The influence of the total biopolymer concentration (0−10% w/w) and SP/GA ratio was represented in the phase diagram. At a total concentration of 0.10%, results were consistent with the turbidity measurement; that is, no phase separation occurred at an SP/GA ratio lower than 1:2 at pH 4.0. Salt effect (NaCl, 0−500 mmol/L) on SP/GA complexes was discussed. Results indicated that SP/GA complexing, which led to the formation of turbidity peaks at pH 3.2, was suppressed when NaCl concentrations were ≥50 mmol/L, whereas the remarkable increase in turbidity around pH 5.0 was caused by the aggregation of soy protein molecules on which gum arabic could be adsorbed.

KEYWORDS: *complex formation, soy protein, gum arabic, charge compensation, phase diagram, protein aggregation*

INTRODUCTION

Protein and polysaccharide are often used in processed food simultaneously. The interactions between protein and polysaccharide play significant roles in controlling the structure, texture, and stability of food systems.[1] The exact pattern of nonspecific protein−polysaccharide interactions (miscibility, complex formation, or thermodynamic incompatibility) is determined by many factors, such as charge density, conformation, and solvent conditions.[2] Complex formation occurs between oppositely charged biopolymers through electrostatic attractions and is widely applied to enzyme immobilization,[3] antigen delivery, protein fractionation,[4,5] and food ingredient encapsulation and stabilization of food products.[6]

Protein−polysaccharide complex results in liquid−liquid phase separation (coacervation) or precipitate-like products in a narrow window of physicochemical conditions, such as pH, ionic strength, and biopolymer ratio.[7] pH determines whether a protein carries a net positive or negative charge and influences the level of protonation/deprotonation of reactive sites along the polysaccharide backbone at the same time.[8] Several critical pH values were found corresponding to the formation of soluble complex (pH_c), the occurrence of phase separation ($pH_{\varphi 1}$), the maximum turbidity (pH_{opt}), and the dissolution of coacervate or precipitate ($pH_{\varphi 2}$).[9−11] Salt also affects complex formation profoundly. At low concentration, salt enhances the protein/polysaccharide complex formation by screening repulsive forces between protein molecules,[12,13] whereas high ionic strength reduces or even suppresses complexing. Weinbreck et al.[12] constructed a binary phase diagram on the conductivity (salt concentration)−polymer concentration plane at fixed pH and protein/polysaccharide ratios to explain the salt effect. In salt-free solution, increase of protein/polysaccharide ratio results in the shift of turbidity curves to higher pH.[11,14] Schmitt et al.[15,16] used ternary phase diagrams to give a general overview of the location and area of the two phases for β-lactoglobulin−acacia gum−water system as a function of polymer concentration and protein/polysaccharide ratio at a fixed pH and salt concentration.

Due to the electrostatic interaction in nature, macromolecular complexing is usually expected to occur through macro ion mutual neutralization. It is true for polyelectrolytes with high charge density. Particularly in the absence of salt, charge-neutral, counterion-free precipitates can be observed when bulk charge stoichiometries equal 1. However, liquid−liquid phase separation (coacervation) can occur when the combined contributions of all ionic species, including small ions, allow for the formation of neutral or near-neutral aggregates. In the food research area, studies on charge stoichiometry for protein−polysaccharide complexing remain scarce. Weinbreck et al.[12] found that pH_{φ} did not change further at a whey protein/EPS B40 ratio of ≥9. At the same time, they determined the electrophoretic mobility under the same pH and found that the mobility ratio for whey protein and EPS B40 was about 1:9−10, thus suggesting an apparent charge

Received: October 16, 2012
Revised: March 28, 2013
Accepted: March 29, 2013
Published: March 31, 2013

stoichiometry of 1:1. Ducel et al.[17] found that a 50:50 mixture of pea protein/arabic gum of equally concentrated solutions formed coacervate particles at pH 3.5. To study the charge relationships of the two macromolecules, they used soft particle analysis theory to calculate charge density (ZN) from electrophoretic mobilities and found that, at pH 3.5, ZN values for pea protein and arabic gum were oppositely signed and had the same absolute value.

Soy proteins are very important ingredients in the food industry, the major components of which are 11S (glycinin) and 7S (β-conglycinin) globulins. Several studies have reported the associative interaction between soy protein and polysaccharide, such as soy protein isolate−pectin interaction in acid protein beverage[18,19] and soy protein isolate−chitosan coacervation.[20] The work by Xia et al.[21] on a soy protein isolate/gum arabic system is mainly focused on its microencapsulation use in embedding sweet orange oil. Gum arabic is an arabinogalactan-type polysaccharide, which is composed of six carbohydrate moieties and a protein fraction and can be considered as a weak polyelectrolyte having a charge density that is pH-dependent. This study was conducted to advance our understanding of SP/GA complexing behavior by investigating the effects of pH, SP/GA ratio, and NaCl concentration (C_{NaCl}) on complex formation, examining the electrophoretic mobility of SP/GA coacervation, and building a SP−GA−water ternary phase diagram. Two aspects were focused on in the study: the charge compensation between the two macromolecules and the aggregation of protein at elevated salt concentration.

MATERIALS AND METHODS

Materials. Hexane-defatted and flush-desolventized soy flake, provided by Shandong Wanderful Industrial & Commercial Co. Ltd., had a protein content of 52.4% (N × 6.25, dry base) and a nitrogen solubility index (NSI) of 85%.

To prepare soy protein with high solubility, the method of Li et al.[22] was used. Briefly, defatted soy flake, which had been prewashed with aqueous alcohol, was suspended in distilled water (pH 7.0) and stirred for 1 h at room temperature (25 ± 2 °C). The supernatant, which was recovered from the suspension by centrifuging, was precipitated at pH 4.5 and then centrifuged to recover protein. After a washing with distilled water, the protein precipitate was resuspended in distilled water and resolubilized by adjusting the pH to 7.0. A small quantity of insoluble substances was removed by centrifugation at 10000 rpm (10700*g*) for 60 min. Protein solution was then dialyzed and freeze-dried. Proximate analysis showed that the dried powder had protein and ash contents of 92.78% (N × 6.25) and 3.17%, respectively, on a dry basis.

Powder gum arabic (GA, Instant gum AA) was a gift from the Nexira Co. (France), and the composition was 2.19% protein (N × 6.25), 10.72% moisture, and 3.32% ash, and nearly no lipid. Carbohydrate content was determined on the basis of percent differential from 100%. The neutrality point of GA was about 2.3. Chemical analyses on all materials were performed according to AOAC methods 979.09 (crude protein), 925.10 (moisture), 923.03 (ash), and 2003.05 (lipid). All other reagents were of analytical grade.

Preparation of SP and GA Stock Solutions. SP and GA stock solutions were prepared by dispersing a certain amount of biopolymer powder in distilled water under gentle stirring at room temperature (25 ± 1 °C) for 2 h and left overnight at 4 °C to allow complete hydration of macromolecules. SP and GA suspensions were centrifuged at 19000 rpm (29500*g*) for 30 min at 4 °C, and the supernatants were filtered through a 0.45 μm membrane. NaN_3 (0.02% w/v) was added to inhibit bacteria growth.

Mixtures of SP and GA were prepared by adding SP solution to GA solution at desired ratios, with distilled water to achieve a total biopolymer concentration (C_p = 0.10%) (adjusted to pH 7.0 with 0.1 and 1 M NaOH). The blend was gently stirred for 30 min. Biopolymer concentrations used in this study reflected the protein (SP) or carbohydrate (GA) equivalent powder weight.

Turbidity Analysis. Turbidity titration upon acidification was measured using a UV−vis spectrophotometer (Shimadzu, Japan) at 600 nm with plastic cuvettes (1 cm path length), from pH 7.0 to 2.0. The mixture was first acidified by adding 0.10% (w/v) glucono-δ-lactone (GDL, purchased from Sigma) to bring the pH to 4.0, followed by the dropwise addition of HCl with a gradient of concentrations: 0.1 mol/L HCl for pH >3.5; 1.0 mol/L HCl for the pH range of 2.7−3.5; and 6 mol/L HCl for the pH range of 2.0−2.7. In this way, the added volume could be controlled in the range of 1.5−3% of total volume; thus, the dilution effect was not significant. Titrations were carried out at 25.0 ± 1.0 °C, and the pH (±0.01 pH unit) was monitored with a Mettler Toledo Delta 320 pH-meter that had been carefully calibrated. Turbidity titrations were also conducted by varying the SP/GA ratio (1:4−8:1 w/w) and in the presence of NaCl (0−500 mmol/L). All measurements were made in triplicate, using separate stock solutions.

Electrophoretic Mobility Determination. Ohshima's soft particle electrophoresis theory[23−25] was applied to determine the charge density (ZN, mol/L) of SP and GA, respectively. The electrophoretic mobilities of SP and GA in solution (0.05% w/v) were determined at different salt concentrations (0.02, 0.04, 0.06, 0.08, and 0.10 mol/L, respectively) and at 25.0 ± 0.1 °C, using a Zetasizer Nano ZS instrument (Malvern, IK). All measurements were made in duplicate. Electrophoretic mobilities were plotted versus salt concentration and were fitted with a model in which ZN was the adjustable parameter.

The electrophoretic mobility (μ) of a soft particle is expressed as

$$\mu = \frac{\varepsilon_0\varepsilon_r}{\eta} \times \frac{\psi_0/K_m + \psi/\lambda}{1/K_m + 1/\lambda} + \frac{e\mathrm{ZN}}{\eta\lambda^2}$$

in which

$$K_m = \kappa(1 + A^2)^{1/4}$$

$$\kappa = \left(\frac{2z^2e^2n}{\varepsilon_0\varepsilon_r kT}\right)^{1/2}$$

$$\psi_{DON} = \frac{kT}{ze}\ln[A + (A^2 + 1)^{1/2}]$$

$$\psi_0 = \frac{kT}{ze}\left\{\ln[A + (A^2 + 1)^{1/2}] + \frac{1}{A} \times [1 - (A^2 + 1)^{1/2}]\right\}$$

$$\text{and} \quad A = \frac{\mathrm{ZN}}{2zn}$$

Here, μ is the electrophoretic mobility, k is the Boltzmann constant, T is the absolute temperature, η is the viscosity, and z and n are the valence and concentration of bulk ions, respectively. Because NaCl was the electrolyte used, hence z = 1. e is the elementary electric charge, whereas ε_r and ε_0 are the relative permittivity of the electrolyte solution and the absolute permittivity of vacuum, respectively. κ_m is the Debye−Hückel parameter of the surface region, ψ_{DON} is the Donnan potential, and ψ_0 is the potential at the boundary between the surface region and solution.

Composition of SP/GA Dense Phase at Different pH Values. Samples of the 1:1 SP/GA system (C_p = 0.10%) were prepared at various pH values and in the presence of 10 mmol/L of NaCl. After acidification to the desired pH value, the mixtures were centrifuged at 10000 rpm (10700*g*). The dense phase was collected for protein and polysaccharide content measurement using the Kjeldahl method and the phenol−sulfuric colorimetric method, respectively. All measurements were made in duplicate.

SP−GA−Water Ternary Phase Diagram. A ternary phase diagram of SP−GA−water mixtures was established at pH 4.0 and 25 ± 1 °C. The tie-lines, corresponding to the composition of each component in the two phases at the thermodynamic equilibrium, were

determined first. Binodal was obtained by connecting the tie-line's end points. To obtain the results, certain amounts of SP and GA solutions, with different SP/GA mixing ratios and total biopolymer concentrations, were mixed into screw-capped plastic tubes. The mixtures were left at 25 ± 1 °C for 2 days to reach equilibrium. The two phases were separated; then the supernatant was poured out and collected. Both separated phases were weighed to determine the wet mass fraction of each phase. Water, SP, and GA contents were determined in the supernatant and the dense lower phase. The water content in the supernatant was evaluated by drying the sample to constant weight at 103 ± 2 °C, whereas that in the dense phase was determined by weighing the phases before and after freeze-drying. The GA content was determined by using the phenol–sulfuric colorimetric method, and the Kjeldahl method was used for SP determination.

The spinodal line, which corresponded to the connection of the phase separation points, was determined by mutual titration of SP and GA solutions (at the same wt % concentration). The phase separation points were determined by the appearance of turbidity on the basis of a 10% increase of optical density as recorded at 600 nm using an UV–vis spectrophotometer (Shimadzu, Japan) with a 1 cm pathway. The amounts of SP and GA solutions used were determined by volume, from which the weight percent biopolymer concentrations were calculated.

RESULTS AND DISCUSSION

pH Titration Turbidity Curve for SP/GA Complex formation. SP/GA complex formation was studied as a function of pH at a 1:1 SP/GA ratio (C_p = 0.10% w/v) in the absence of NaCl. As shown in Figure 1, acidification of SP/GA mixture from neutral pH first led to the formation of soluble complexes at pH 4.40 ± 0.00. This point was defined as pH_c, which signified the initial experimentally detectable attraction between protein and polysaccharide. Above pH_c, electrostatic repulsive forces prohibited the formation of complexes, and the optical density (OD_{600}) remained at the baseline. With further acidification to pH 3.55 ± 0.11 ($pH_{\varphi 1}$), an abrupt increase in OD_{600} was observed, indicating the formation of insoluble complex particles. OD_{600} rose to the maxima at pH 3.15 ± 0.02 (pH_{opt}) and decreased rapidly as the pH continued to drop. At pH 2.30 ± 0.02 ($pH_{\varphi 2}$), complete dissolution of insoluble complex was assumed to occur because the OD_{600} was very low and both biopolymers began to carry a similar net charge. Liu et al.[14] studied the pea protein isolate/gum ababic complex coacervation and reported a quite similar pH titration turbidity curve for the 1:1 mixture. The critical pH values (pH_c, $pH_{\varphi 1}$, pH_{opt}, and $pH_{\varphi 2}$) were found to be 4.2, 3.7, 3.5, and 2.6, respectively. Moreover, canola protein isolate–alginate,[26] lentil protein isolates–gum arabic,[27] and pea protein isolate–chitosan[28] systems all displayed similar pH titration curves.

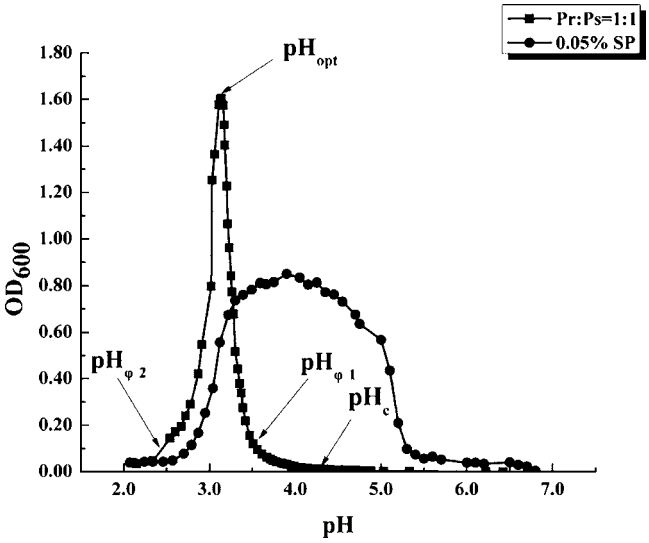

Figure 1. Turbidity curves for the SP/GA system (C_p = 0.10%, Pr:Ps = 1:1) and homologous SP solution as a function of pH, in the absence of NaCl. The values of pH_c, $pH_{\varphi 1}$, and $pH_{\varphi 2}$ were determined graphically as the intersection point of two tangents to the curve, whereas pH_{opt} corresponded to the maximum optical density at 600 nm.

Acidification of GA solution alone did not induce visible OD_{600} change (not shown), but soy protein displayed a remarkable turbidity increase during acidification (Figure 1). The drastic OD_{600} increase of the SP/GA mixture at $pH_{\varphi 1}$ indicated a phase transition like behavior, whereas the gradual OD_{600} change in SP solution was caused by protein aggregation. It seemed that the aggregation of soy protein was suppressed in the SP/GA mixture because no such gradual turbidity increase was observed between pH 6.5 and 4.4 in the SP/GA mixture (Figure 1). Moreover, the OD_{600} curve of SP alone and that of the mixture were overlapped within the range of pH 3.5–2.0. It could be presumed that complexes were formed between GA chains and small soy protein aggregates rather than individual SP molecules. Liu et al.[14] and Ayree et al.[27] considered protein aggregates were participated in complex formation in different protein–polysaccharide mixtures.

Complex Formation at Different SP/GA Ratios. The effect of SP/GA ratio (1:4–8:1 w/w, C_p = 0.10% w/v) on complex coacervation was investigated in the absence of salt. As Figure 2 presents, an increase in SP/GA ratio from 1:4 to 8:1 shifted the turbidity curves to higher pH. Similar shifts of turbidity curves were also reported by Weinbreck et al.[12] and Liu et al.[14] The lower OD_{600} at lower SP/GA ratio (1:4 and 1:2) corresponded to lower insoluble complex volume, which could be attributed to the smaller molecular volume of the gum arabic chain at lower pH. A pronounced plateau was observed for turbidity curves of 2:1, 4:1, and 8:1 SP/GA mixtures at pH < pH_{opt}, which could result from the aggregation of acid-denatured soy proteins. Ayree et al.[27] carried out a similar

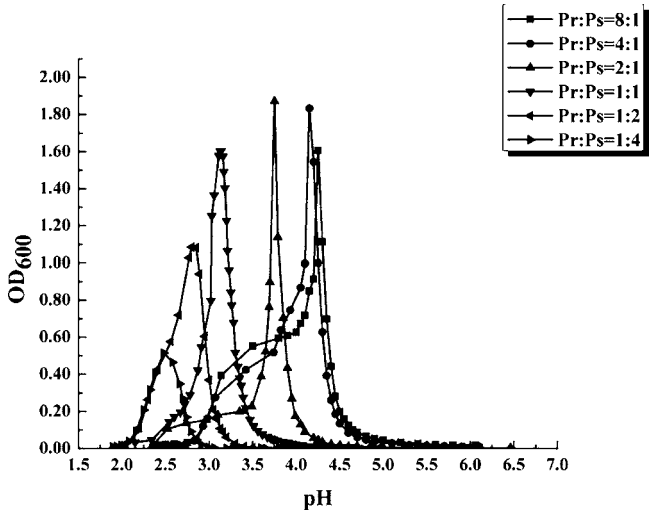

Figure 2. Turbidity curves for SP/GA systems as a function of SP/GA ratio (C_p = 0.10%) in the absence of NaCl.

dx.doi.org/10.1021/jf400305z | J. Agric. Food Chem. 2013, 61, 3934–3940

turbidimetric analysis as a function of pH and Pr:Ps ratio to find a small plateau when lentil protein isolate/gum arabic ratios were 1:1 and 1.5:1. The authors reasoned that the plateau was associated with enhanced stabilizing hydrophobic interactions occurring within the lentil protein aggregates. Increase of the SP/GA ratio from 4:1 to 8:1 resulted in a much smaller change in critical pH values (Figure 2). Liu et al.[14] found similar results for a pea protein isolate/gum arabic system, showing the critical pH values were stable when the mixing ratio was 4:1.

To know whether the shifts of critical pH values as the SP/GA ratios increased could be related to the charge compensation of SP and GA, the charge densities (ZN) for SP and GA were determined respectively at different pH values.

The electrophoretic mobilities of GA and SP at different pH values as a function of NaCl concentration are shown in Figure 3. For both macromolecules, the absolute values of electrophoretic mobility decreased with increasing ionic concentration. The leveling off of electrophoretic mobilities toward nonzero values allowed us to conclude that both macromolecules could be considered as "soft particles", and ZN, the charge density of biopolymers, was calculated (Table 1). It could found that for SP, a lower ZN value was obtained at pH values closer to the isoelectric point (pH 4.5). On the contrary, for GA, the absolute value of ZN should likely be larger at high pH because the neutralization point giving a zero electrophoretic mobility was about pH 2.3.

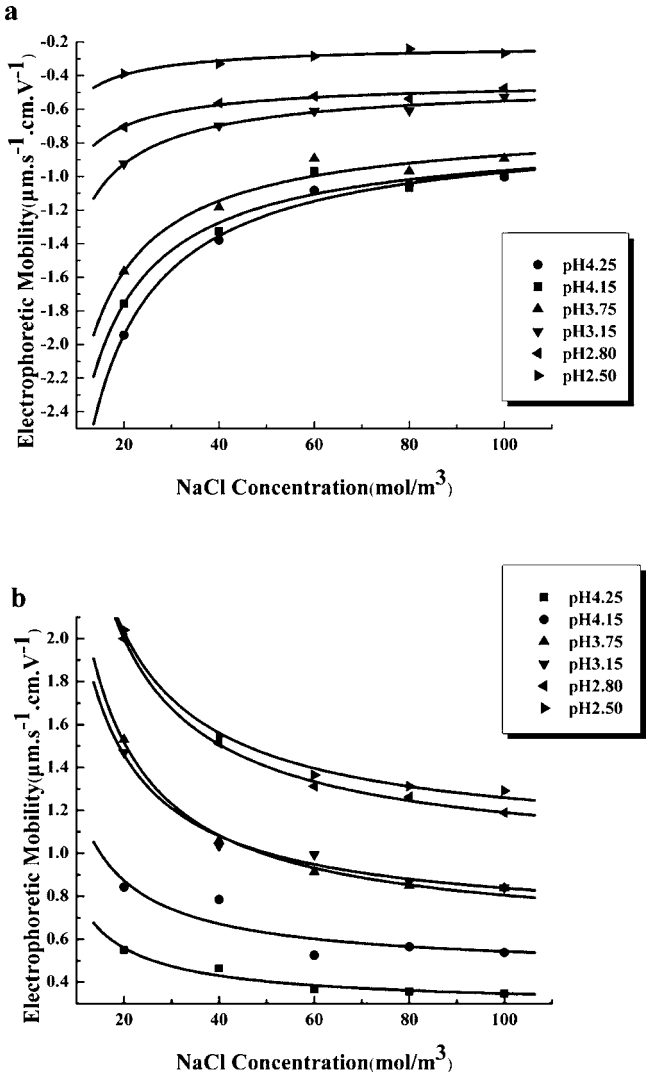

Figure 3. Electrophoretic mobility for GA (a) and SP (b) at different pH values.

Table 1. Determination of the Surface Charge Properties of SP and GA in Solution Using Ohshima's Method

pH		ZN (mol/L)	R^2
4.25	GA	−0.03668	0.997
	SP	0.00908	0.999
4.15	GA	−0.03568	0.988
	SP	0.01042	0.712
3.75	GA	−0.02472	0.938
	SP	0.02586	0.991
3.15	GA	−0.01315	0.976
	SP	0.02600	0.966
2.80	GA	−0.00695	0.933
	SP	0.02840	0.998
2.50	GA	−0.00474	0.886
	SP	0.02939	0.982

The charge density ratio α was defined as

$$\alpha = \rho \times |ZN(GA)|/ZN(SP)$$

where ρ is the reciprocal of the SP/GA ratio (mass ratio), |ZN(GA)| is the absolute value of the ZN for GA, and ZN(SP) is ZN for SP. Interestingly, it was found that ln α was linear with pH (R^2 = 0.970). A series of parallel lines that crossed over the pH axis (i.e., ln α = 0) at different pH values were obtained for different ρ values (Figure 4a). With the increase of ρ, the pH at which ln α = 0 was shifted to lower pH. Then, pH values corresponding to α = 1(i.e., ln α = 0, $pH_{\alpha=1}$), $pH_{\varphi 1}$ for different SP/GA ratios, and the difference in $pH_{\alpha=1}$ and $pH_{\varphi 1}$ at the same SP/GA ratio ($\Delta pH = pH_{\alpha=1} - pH_{\varphi 1}$) were plotted against the SP/GA ratio (Figure 4b). It could be seen that $pH_{\alpha=1}$ values for different SP/GA ratios were in good agreement with the corresponding $pH_{\varphi 1}$. In other words, the SP/GA mixture of different ratios started to form an insoluble complex at those pH values at which charge compensation conditions were fulfilled. Weinbreck et al.[12] and Burgess et al.[29] also found the apparent charge stoichiometry of 1:1 at pH_{φ} using the ζ-potential ratio and electrophoretic mobility ratio, respectively. Other authors[5,30] also pointed out that the phase separation occurring at pH_{φ} was a consequence of charge neutralization of the complexes.

SP−GA−Water Ternary Phase Diagram. The SP−GA−water ternary phase diagram was built at pH 4.0 as a function of biopolymer concentration and SP/GA ratio (Figure 5). Phase separation was found to be associative in all systems, leading to a concentrated phase and a supernatant phase. The texture of the concentrated phases was "precipitate-like" at higher SP/GA ratio, but "gel-like" at lower SP/GA ratio. The supernatant phase, unlike the concentrated phase, was very dilute and consisted mainly of water and a small amount of excess SP and GA left over after the formation of the complex. At low GA concentrations the composition of the supernatant was close to the SP−water binary. When the bulk GA concentration was increased, the supernatant composition shifted gradually to the GA−water binary.

As Figure 5a illustrated, the binodal curves enclosed a two-phase region in the water corner of the ternary phase diagram, extending toward the SP−GA axis. The two-phase region was drop-shaped, which was generally the case for complex

dx.doi.org/10.1021/jf400305z | J. Agric. Food Chem. 2013, 61, 3934−3940

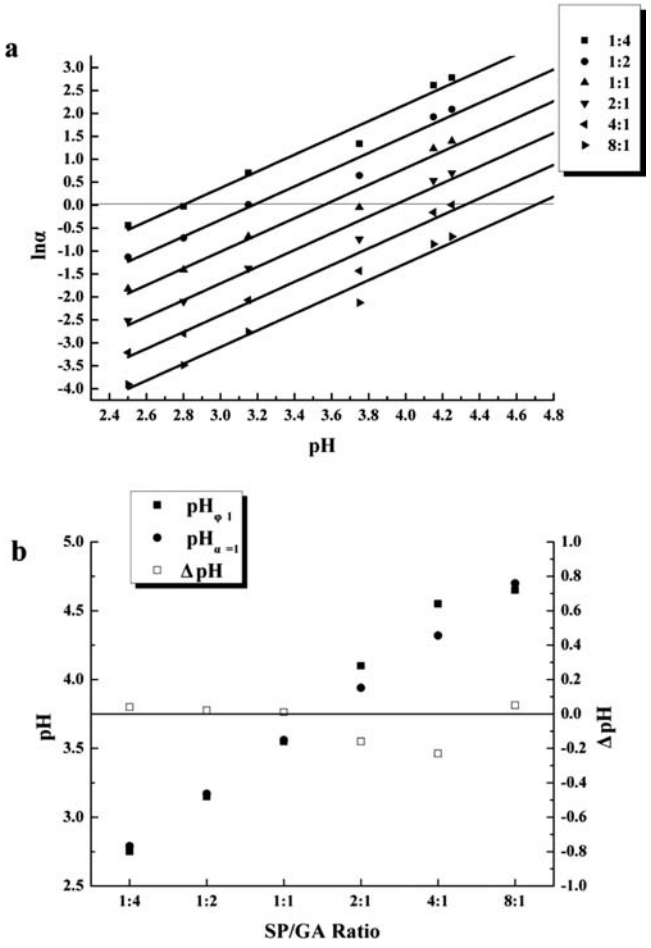

Figure 4. Relationship between ZN values of the two polymers and pH: (a) linear relationship of ln α and pH at different SP/GA ratios; (b) difference in values of $pH_{\alpha=1}$and $pH_{\varphi 1}$, $\Delta pH = pH_{\alpha=1} - pH_{\varphi 1}$.

coacervation.[15,16] The confinement of the two-phase region into the solvent corner typically represented the existence of equilibrium between the supernatant phase (left points of tie-lines) and the concentrated phase (right points of tie-lines).[31] Mixtures with an overall composition within the area enclosed by the binodal curve were thermodynamically unstable. The appearance of a single phase at high GA or SP concentration was described as redissolution of the complex due to excess binding of the oppositely charged GA, leading to charge reversal and hence greater solubility.

Experimental spinodals for the total polymer concentrations of 1, 2, 5, and 10% (w/v) are presented in Figure 5b. The upper limit of the two-phase region was adjacent to the SP axis, whereas the lower limit was far from the water axis. This indicated that a certain amount of GA solution could dissolve relatively large amounts of SP solution before phase separation. By contrast, phase separation occurred instantly upon addition of a small amount of GA solution into an SP one. Therefore, the two-phase region was asymmetrical, which was closer to the SP axis compared to the water axis. Schmitt et al.[15,16] found that the lower limit was far from the axis compared to the upper one in a β-lactoglobulin−acacia gum−water ternary phase diagram. They thought greater amounts of a protein solution with lower electrophoretic mobility were required to neutralize an acacia gum solution.

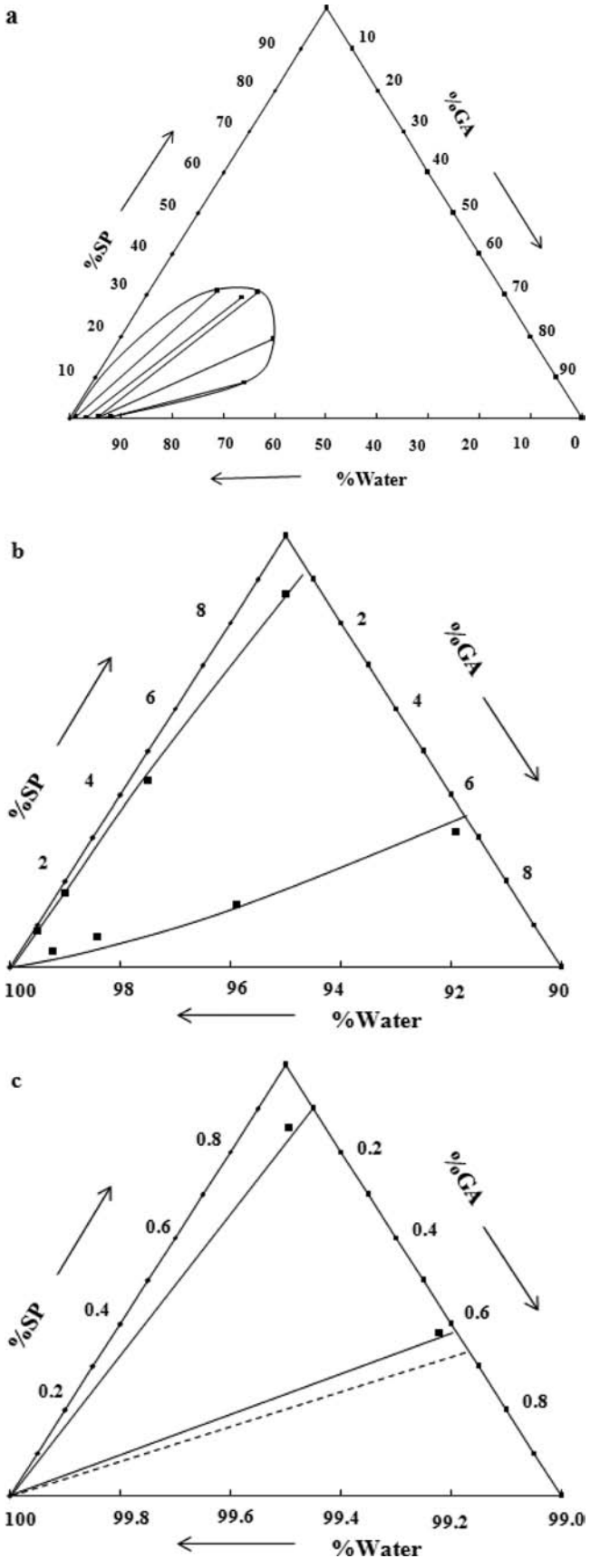

Figure 5. Ternary phase diagrams of SP−GA−water systems at pH 4.0: (a) tie-lines and binodal curve; (b) spinodal lines for 0−10% polymer concentration; (c) spinodal lines for 0−1% polymer concentration. Results are expressed in percentages.

dx.doi.org/10.1021/jf400305z | J. Agric. Food Chem. 2013, 61, 3934−3940

The angular trisection of the SP−water corner (dashed line in Figure 5c), on which the SP/GA ratios were all 1:2, was located under the lower limit of experimental spinodals, indicating that this line was in the one-phase region of the phase diagram. This result was consistent with Figure 2, in which we can learn that there was no phase separation at pH 4.0 for SP/GA = 1:2 or lower when C_p = 0.10% (w/v). In a similar way, a two-phase area was correctly predicted in the region above the angle bisector where SP/GA ratios were 1:1 and higher.

Effect of Salt Concentration on SP/GA Complex Formation. SP/GA complexing under different salt concentrations was investigated at SP/GA = 1:1 and C_p = 0.10%, as shown in Figure 6. At C_{NaCl} = 2.5 and 5 mmol/L, pH titrations

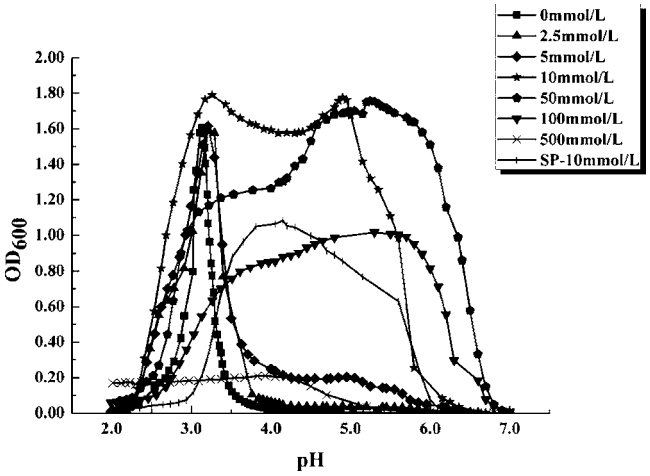

Figure 6. Turbidity curves for SP/GA systems (C_p = 0.10%, Pr:Ps = 1:1) at different NaCl concentrations and 0.05%SP solution only at C_{NaCl} = 10 mM.

gave similar turbidity curves with pH_{opt} at almost the same position (pH ~3.2) as that in the absence of NaCl except $pH_{\varphi 1}$ was shifted to a higher pH. When C_{NaCl} was ≥5 mmol/L, turbidity at high pH was observed and increased dramatically. The turbidity−pH profile for C_{NaCl} of 10 mmol/L was totally different, which exhibited a broad plateau rather than a sharp peak. In Figure 7, optical densities at pH 3.2 and 5.0 were investigated as a function of C_{NaCl}. The addition of salt to the SP/GA mixture decreased OD_{600} at pH 3.2 after an initial stagnant period at $C_{NaCl} \leq$ 10 mmol/L. At pH 5.0, however, OD_{600} increased rapidly with the introduction of NaCl to the SP/GA mixture until a maximal OD_{600} was reached, almost the same value as that at pH 3.2, at C_{NaCl} = 10 and 50 mmol/L (Figure 7). It could be found that the OD_{600} curve for the SP/GA mixture at pH 5.0 behaved like that at pH 3.2 in terms of OD_{600} value, but it was more similar to the curve for homologous SP solution on considering the maximal C_{NaCl} at which OD_{600} began to be decreased. The difference in the molecular interaction pattern at pH 5.0 and 3.2 was further exemplified by composition analysis of the dense phase. As shown in Table 2, although the initial GA and SP concentrations in mixed solutions were the same, the actual GA and SP contents in the dense phase were very different. The actual SP/GA ratio in the dense phase for pH 3.2 was nearly 1:1, but that for pH 5.0 was more than 4:1.

Weinbreck et al.[12] studied the effect of ionic strength on complex coacervation of whey protein/gum arabic mixture and

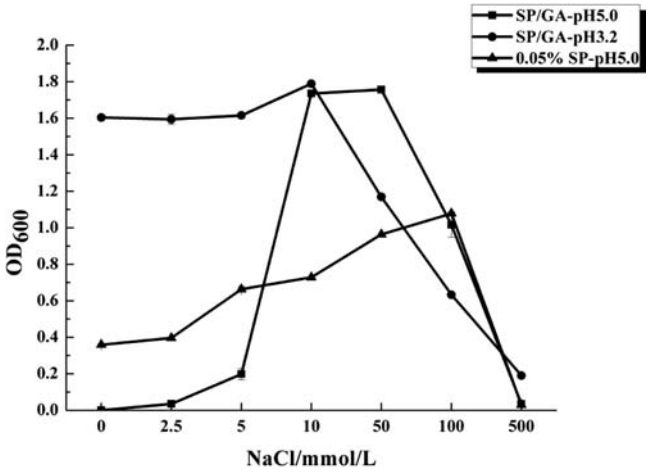

Figure 7. Turbidity curves of SP/GA mixtures, SP/GA = 1, C_p = 0.10%, and homologous SP solution as a function of NaCl concentration.

Table 2. Biopolymer Composition of the SP/GA Dense Phase at Different pH Values (C_{NaCl} = 10 mM, Dry Basis)

pH	SP (%)	GA (%)
3.2	54.43 ± 0.01	43.42 ± 0.01
5.0	81.71 ± 0.01	11.42 ± 0.01

found that $pH_{\varphi 1}$, pH_{opt}, and turbidity decreased as the salt concentration increased. Wang et al.[32] reported that pH_{φ} of a β-lactoglobulin/pectin system shifted moderately to a higher value when the salt concentration was increased from 0.01 to 0.1 M, but shifted to a lower value when the salt concentration was >0.2 M. They did not find a suppression on optical density even when C_{NaCl} was 0.8 M. However, the authors found that β-lactoglobulin per se gave almost the same turbidity and thus concluded that protein self-aggregation played the predominant role in their systems. Neither of them reported the formation of insoluble particles at pH range above the p*I* of the protein.

The turbidity peak at pH 3.2 appeared to be attributable to SP/GA complex formation, which was substantially suppressed at $C_{NaCl} \geq$ 50 mmol/L (Figures 6 and 7). Formation of insoluble substance at high pH could be related to the abnormal salt-dependent variation in the aggregation of soy protein.[33] Instead of being "salted in" as most proteins behaved, soy proteins were "salted out" at low salt concentration, resulting in the OD_{600} being increased at $C_{NaCl} \leq$ 100 mmol/L (Figure 7). Kumosinski[34] believed that the aggregation could be linked to the free energy of salt binding on soy protein. The adsorption of a small amount of GA, the chain of which was highly extended at high pH, on the "positive patch" of protein molecules resulted in particles with larger volume. This could explain why the turbidity was much higher than that for SP alone. At C_{NaCl} = 100 and 500 mmol/L, the OD_{600} for SP/GA mixture was exactly like that for SP alone at pH 5.0. This indicated that only SP aggregates contributed to the OD_{600} at these salt concentrations, and the GA adsorption was suppressed completely.

In summary, soy protein/gum arabic mixture formed complexes at zero added salt, which could be followed by turbidity measurement during pH titration. The charge compensation was found at the incipient point of insoluble complex formation ($pH_{\varphi 1}$) by comparing charge densities (ZN) of two macromolecules. A soy protein−gum arabic−

dx.doi.org/10.1021/jf400305z | J. Agric. Food Chem. 2013, 61, 3934−3940

water ternary phase diagram gave an overview of the location and area of the two phases at pH 4.0 as a function of biopolymer concentration and mixing ratio. Salt addition caused a substantial turbidity increase at pH values higher than the isoelectric point of soy protein, which could be related to the abnormal aggregation behavior of soy proteins at low salt concentration.

AUTHOR INFORMATION

Corresponding Author

*E-mail: yfhua@jiangnan.edu.cn.

Notes

The authors declare no competing financial interest.

REFERENCES

(1) Schmitt, C.; Turgeon, S. L. Protein/polysaccharide complexes and coacervates in food systems. *Adv. Colloid Interface Sci.* **2011**, *167*, 63−70.

(2) Doublier, J. L.; Garnier, C.; Renarda, D.; Sanchez, C. Protein−polysaccharide interactions. *Curr. Opin. Colloid Interface Sci.* **2000**, *5*, 202−214.

(3) Xia, J.; Mattison, K.; Romano, V.; Dubin, P. L.; Muhoberac, B. B. Complexation of trypsin and alcohol dehydrogenase with poly-(diallyldimethylammonium chloride). *Biopolymers* **1997**, *41*, 359−365.

(4) Wang, Y.; Gao, J. Y.; Dubin, P. L. Protein separation via polyelectrolyte coacervation: selectivity and efficiency. *Biotechnol. Prog.* **1996**, *12*, 356−362.

(5) Xu, Y.; Mazzawi, M.; Chen, K. Protein purification by polyelectrolyte coacervation: influence of protein charge anisotropy on selectivity. *Biomacromolecules* **2011**, *12*, 1512−1522.

(6) Giroux, H. J.; Britten, M. Encapsulation of hydrophobic aroma in whey protein nanoparticles. *J. Microencapsulation* **2011**, *5*, 337−343.

(7) de Kruif, C. G.; Weinbreck, F.; de Vries, R. Complex coacervation of proteins and anionic polysaccharides. *Colloid Interface Sci.* **2004**, *9* (5), 340−349.

(8) Ye, A. Complexation between milk proteins and polysaccharides via electrostatic interactions: principles and applications: a review. *Int. J. Food. Sci. Technol.* **2008**, *43*, 406−415.

(9) Ru, Q.; Wang, Y.; Lee, J.; Ding, Y.; Huang, Q. Turbidity and rheological properties of bovine serum albumin/pectin coacervates: effect of salt concentration and initial protein/polysaccharide ratio. *Carbohydr. Polym.* **2012**, *88*, 838−846.

(10) Liu, S.; Cao, Y. L.; Ghosh, S. Intermolecular interactions during complex coacervation of pea protein isolate and gum arabic. *J. Agric. Food Chem.* **2010**, *58*, 552−556.

(11) Weinbreck, F.; Nieuwenhuijse, H.; Robijn, G. W.; de Kruif, C. G. Complexation of whey proteins with carrageenan. *J. Agric. Food Chem.* **2004**, *52* (11), 3550−3555.

(12) Weinbreck, F.; Nieuwenhuijse, H.; Robijn, G. W.; de Kruif, C. G. Complex formation of whey proteins: exocellular polysaccharide EPS B40. *Langmuir* **2003**, *19* (22), 9401−9410.

(13) Seyrek, E.; Dubin, P. L.; Tribet, C.; Gamble, E. A. Ionic strength dependence of protein-polyelectrolyte interactions. *Biomacromolecules* **2003**, *4* (2), 273−282.

(14) Liu, S.; Low, N. H.; Nickerson, M. T. Effect of pH, salt, and biopolymer ratio on the formation of pea protein isolate-gum arabic complexes. *J. Agric. Food Chem.* **2009**, *57*, 1521−1526.

(15) Schmitt, C.; Sanchez, C.; Despond, S.; Renard, D.; Thomas, F.; Hardy, J. Effect of protein aggregates on the complex coacervation between β-lactoglobulin and acacia gum at pH 4.2. *Food Hydrocolloids* **2000**, *14* (4), 403−413.

(16) Schmitt, C.; Sanchez, C.; Thomas, F.; Hardy, F. Complex coacervation between β-lactoglobulin and acacia gum in aqueous medium. *Food Hydrocolloids* **1999**, *13* (6), 483−496.

(17) Ducel, V.; Saulnier, P.; Richard, J.; Boury, F. Plant protein−polysaccharide interactions in solutions: application of soft particle analysis and light scattering measurements. *Colloids Surf., B: Biointerfaces* **2005**, *41*, 95−102.

(18) Lam, M.; Shen, R.; Paulsen, P.; Corredig, M. Pectin stabilization of soy protein isolates at low pH. *Food Res. Int.* **2007**, *40*, 101−110.

(19) Jaramillo, D. P.; Roberts, R. F.; Coupland, J. N. Effect of pH on the properties of soy protein−pectin complexes. *Food Res. Int.* **2011**, *44*, 911−916.

(20) Yuan, Y.; Wan, Z.-L.; Yin, S.-W.; Yang, X.-Q.; Qi, J.-R.; Liu, G.-Q.; Zhang, Y. Characterization of complexes of soy protein and chitosan heated at low pH. *Food Sci. Technol.* **2013**, *50*, 657−664.

(21) Xia, X. J.; Yan, Y. H.; Jian, Y. Microencapsulation of sweet orange oil by complex coacervates with soybean protein isolate/gum arabic. *Food Chem.* **2011**, *125*, 1267−1272.

(22) Li, X.; Li, Y.; Hua, Y.; Qiu, A.; Yang, C.; Cui, S. Effect of concentration, ionic strength and freeze-drying on the heat-induced aggregation of soy proteins. *Food Chem.* **2007**, *104*, 1410−1417.

(23) Ohshima, H. Electrophoretic mobility of soft particles. *Colloids Surf., A: Physicochem. Eng. Aspects* **1995**, *103*, 249−255.

(24) Ohshima, H. *Electrical Phenomena at Interfaces*, 2nd ed.; Ohshima, H., Furusawa, K., Eds.; Dekker: New York, 1998.

(25) Ohshima, H.; Nakamura, M.; Kondo, T. Electrophoretic mobility of colloidal particles coated with a layer of adsorbed polymers. *Colloid Polym. Sci.* **1992**, *270*, 873−877.

(26) Klassen, D. R.; Elmer, C. M.; Nickerson, M. T. Associative phase separation involving canola protein isolate with both sulphated and carboxylated polysaccharides. *Food Chem.* **2011**, *126*, 1094−1101.

(27) Aryee, F. N. A.; Nickerson, M. T. Formation of electrostatic complexes involving mixtures of lentil protein isolates and gum arabic polysaccharides. *Food Res. Int.* **2012**, *48*, 520−527.

(28) Elmer, C.; Karaca, A. C.; Low, N. H.; Nickerson, M. T. Complex coacervation in pea protein isolate-chitosan mixtures. *Food Res. Int.* **2011**, *44*, 1441−1446.

(29) Burgess, D. J.; Carless, J. E. Microelectrophoretic studies of gelatin and acacia for the prediction of complex coacervation. *J. Colloid Interface Sci.* **1984**, *98* (1), 1−8.

(30) Kayitmazer, A. B.; Bohidar, H. B.; Mattison, K. W.; Bose, A.; Sarkar, J.; Hashidzume, A.; Russo, P. S.; Jaeger, W.; Dubin, P. L. Mesophase separation and probe dynamics in protein−polyelectrolyte coacervates. *Soft Matter* **2007**, *3*, 1064−1076.

(31) Wang, J.; Cohen Stuart, M. A.; van der Gucht, J. Phase diagram of coacervate complexes containing reversible coordination structures. *Macromolecules* **2012**, *45*, 8903−8909.

(32) Wang, X.; Wang, Y.; Ruengruglikit, C.; Huang, Q. Effects of salt concentration on formation and dissociation of β-lactoglobulin/pectin complexes. *J. Agric. Food Chem.* **2007**, *55*, 10432−10436.

(33) Shen, J. L. Solubility profile, intrinsic viscosity, and optical rotation studies of acid precipitated soy protein and of commercial soy isolate. *J. Agric. Food Chem.* **1976**, *24* (4), 784−788.

(34) Kumosinski, T. F. Use of thermodynamic linkage to study the salt-induced solubility change of soybean isolate. *J. Agric. Food Chem.* **1988**, *36*, 669−672.